2018-05

On the Enigma of Glutathione-Dependent Styrene Degradation in Gordonia rubripertincta CWB2

Heine, T

10.1128/AEM.00154-18
APPLIED AND ENVIRONMENTAL MICROBIOLOGY

This is an accepted manuscript of an article published by Highwire in Applied and Environmental Microbiology (accepted February 23 2018) available at:
https://doi.org/10.1128/AEM.00154-18.

==========

On the enigma of glutathione dependent styrene degradation in *Gordonia rubripertincta* CWB2

Thomas Heine[1,#], Juliane Zimmerling[1], Anne Ballmann[1], Sebastian Bruno Kleeberg[1], Christian Rückert[2], Tobias Busche[2], Anika Winkler[2], Jörn Kalinowski[2], Ansgar Poetsch[3,4], Anika Scholtissek[1], Michel Oelschlägel[1], Gert Schmidt[5] and Dirk Tischler[1,6,#]

[1]Institute of Biosciences, TU Bergakademie Freiberg, Leipziger Str. 29, Freiberg, Germany.

[2]Technologieplattform Genomik, Centrum für Biotechnologie (CeBiTec), Universität Bielefeld, Universitätsstr. 27, Bielefeld, Germany.

[3]Plant Biochemistry, Ruhr University Bochum, 44801 Bochum, Germany

[4]School of Biomedical and Healthcare Sciences, Plymouth University, Plymouth PL4 8AA, UK

[5]Institut für Keramik, Glas- und Baustofftechnik, TU Bergakademie Freiberg, Agricolastr. 17, Freiberg, Germany.

[6]Microbial Biotechnology, Ruhr University Bochum, 44801 Bochum, Germany

[#]For correspondence. E-mail heinet@tu-freiberg.de, dirk-tischler@email.de; Tel. +49 3731 392103.

Running title: Styrene degradation via glutathione-*S*-transferase

ABSTRACT

Among bacteria, only a single styrene specific degradation pathway has been reported so far. It comprises the activity of styrene monooxygenase, styrene oxide isomerase and phenylacetaldehyde dehydrogenase yielding phenylacetic acid as central metabolite. The alternative route comprises ring-hydroxylating enzymes and yields vinyl catechol as central metabolite, which undergoes *meta*-cleavage. This was reported to be unspecific and also allows the degradation of benzene derivatives. However, some bacteria had been described to degrade styrene but do not employ one of those routes or only parts of them. Herein we describe a novel “hybrid” degradation pathway for styrene located on a plasmid of foreign origin. As putatively also unspecific, it allows metabolizing chemically analogous compounds (e.g. halogenated and/or alkylated styrene derivatives). *Gordonia rubripertincta* CWB2 was isolated with styrene as sole source of carbon and energy. It employs an assembled route of the styrene side chain degradation and isoprene degradation pathways that also funnels into phenylacetic acid as central metabolite. Metabolites, enzyme activity, genome, transcriptome and proteome data reinforce the observation and allow to understand this biotechnologically relevant pathway which can be used for the production of ibuprofen.

IMPORTANCE

Degradation of xenobiotics by bacteria of high interest for bioremediation, but also as involved enzymes are potential catalysts in biotechnological applications. This study reveals a novel degradation pathway for the hazardous organic compound styrene in *Gordonia rubripertincta* CWB2. It is an impressive illustration of horizontal gene transfer, which enables novel metabolic capabilities. This study presents glutathione-dependent styrene metabolization in an (actino-)bacterium. Further, the

genomic background of the ability of strain CWB2 to produce ibuprofen is demonstrated.

INTRODUCTION

Styrene is a monoaromatic compound that naturally occurs as a component of tar, volatile and oily substances from plants and food, but can also be produced by microorganisms. Styrene is of high relevance in industry and produced in million tonne scale causing substantial anthropogenic release. This is problematic as it is hazardous for living organisms (1–3). Due to the disposability, it is corollary that organisms evolved strategies to detoxify and/or use styrene as a source of energy and carbon (3–5).

Styrene can be channelled through different unspecific degradation pathways due to relaxed substrate specificity of the respective enzymes (see supplemental material and 3 for details). However, only one styrene specific degradation pathway is known and seems to be favoured by microorganisms under aerobic conditions (3, 5, 6). This upper degradation pathway is initiated by oxidation of the vinyl side chain. A styrene monooxygenase (SMO) produces *(S)*-styrene oxide, which is converted by a membrane bound styrene oxide isomerase (SOI) to phenylacetaldehyde. A phenylacetaldehyde dehydrogenase (PAD) oxidizes the aldehyde to phenylacetic acid (PAA) (7). PAA is a central catabolite and metabolized in the so-called lower degradation pathway, which is present in about 16% of all genome-sequenced microorganisms (8, 9). That route has been described for several proteobacteria (*Pseudomonas*, *Xanthobacter*, *Sphingopyxis*), actinobacteria (*Rhodococcus*, *Corynebacterium*) and fungi (*Exophiala*) (reviewed by 3).

Rhodococcus sp. ST-10 has an incomplete degradation cluster lacking the SOI,

while still being able to use styrene as sole source of carbon and energy (10–13). This gene cluster comprises the SMO and a putative (partial) open reading frame (ORF), designated as “ORF3”. It was hypothesized that the SOI can be bypassed by chemical conversion of styrene oxide to phenylacetaldehyde or enzymatically (12–14). However, chemical conversion is unlikely and no probable enzymes were identified (3), thus the degradation pathway for strain ST-10 remains unclear.

The genus *Gordonia* is known to be a versatile degrader of aromatic compounds (15, 16) and *Gordonia rubripertincta* CWB2 in particular is able to metabolize styrene and related compounds. As previously described, strain CWB2 was obtained from a soil sample and separated via styrene-enrichment culture (17–19). Moreover, it was shown that it is able to produce ibuprofen from 4-isobutyl-α-methylstyrene in a co-metabolic process (17, 18). Oelschlägel *et al.* 2015 reported that other styrene degraders are not capable to catalyze this reaction and therefore proposed substantial differences in the respective enzymatic cascades. Interestingly, *Gordonia rubripertincta* CWB2 has a cluster that is homolog to the partial one of strain ST-10.

In this study, we identified the complete gene cluster, which enables styrene degradation in strain CWB2. Therefore, we studied the transcriptome and the proteome under styrene exposure. Further, we measured the activity of key enzymes to clarify the root of the metabolic potential of *Gordonia rubripertincta* CWB2. Moreover, this gene cluster seems to be alien as it is located on a plasmid and assigned as genomic island if compared to the rest of the genome. It embodies a hybrid of several homolog epoxide and aromatic compound degradation clusters from different actinobacteria.

RESULTS

Identification and annotation of gene clusters associated with styrene degradation. Genes that might be involved in styrene degradation in *G. rubripertincta* CWB2 were identified and annotated by homology search using the BLASTP algorithm (20) on the non-redundant protein database or the UniProtKB database (NCBI). The annotation of the putative styrene degradation cluster with respect to the closest (characterized) homolog is listed in Table 2 and Dataset S1. A 32424-bp cluster with 36 putative open reading frames (*orf*) was identified on the plasmid pGCWB2 (~ 100 kbp), which is framed by a styrene monooxygenase (*GCWB2_24100*) and phenylacetaldehyde dehydrogenase (*GCWB2_23925*). Interestingly, the average GC content of this cluster is 62.11% and thus 5% lower as for the whole genome. The GC content of the whole plasmid is 3% lower compared to the chromosome. Besides a high amount of hypothetical proteins, pGCWB2 contains 4 transposase-family proteins, 2 integrase-like proteins, one relaxase-like protein and one type IV secretory system as an inventory for gene mobility. Genomic island analysis on the whole genome illustrates that at least parts of this styrene degradation cluster have foreign origin (Fig. 1).

The cluster can be separated into 4 subclusters comprised as follows: cluster S1 contains a styrene monooxygenase, which is known to initiate the styrene degradation at the vinyl side chain. The closest characterized homolog of this protein was found in *Rhodococcus* sp. ST-10 (StyA – 86% identity at amino acid level; StyB – 82%). A phylogenetic analysis of the amino acid sequence classifies it as an E1-type SMO (Fig. S2). The closest match within *Gordonia* species is a putative monooxygenase from *Gordonia polyisoprenivorans* NBRC 16320 (GAB22407 – 45%; GAB22406 – 39%). However, also the genetic organisation refers to a close relation

to the *Rhodococcus* cluster as the partial sequence of ORF_3 from strain ST-10 shows 67% identity to GCWB2_24090. Transmembrane domain prediction (TMHMM) of GCWB2_24090 identified 4 transmembrane helices what classifies this protein as hypothetical membrane associated. Beyond that, no characterized homologs and no known domains are present in the database for this ORF. It has to be mentioned that no styrene oxide isomerase (*styC*) gene was found on the genome of strain CWB2.

The second cluster S2 embeds 7 hypothetical proteins (GCWB2_24085 - GCWB2_24055). Two of them are presumably soluble and the others are annotated as membrane proteins, while each has one transmembrane domain. Members of these clusters appear to be rare within the database and are predominantly present in rhodococci. *Rhodocoocus opacus* 1CP owns a homologous cluster downstream of its StyABCD cluster (WP_065493732 - WP_045063326; 56 - 68%). Further, *Gordonia* sp. i37 has a homologous gene cluster in the neighbourhood of a recently recorded isoprene degradation cluster (contig257: WP_079929940 - WP_079929944, contig258: OPX14963 - OPX14964; 56 - 74%) (21).

Cluster S3 encodes for proteins that might be involved in glutathione and isoprene metabolism. GCWB2_24050 and GCWB2_24045 show highest identity to a glutamate-cysteine ligase GshA (P9WPK7 – 33%) and a glutathione synthetase GshB (P45480 – 50%) followed by a putative coenyzme A-disulfide reductase (CoA-DSR). The other genes of this cluster (*GCWB2_24050* - *GCWB2_24010*) encode for a putative MarR-like transcriptional regulator, a coenzyme A-transferase, a dehydrogenase, a glutathione *S*-transferase, a disulfidebond oxidoreductase and an aldehyde dehydrogenase. The closest characterized homolog of the latter gene product is the phenylacetaldehyde dehydrogenase from *Pseudomonas fluorescens* ST (O06837 – 36%). Cluster S3 can also be found in *Aeromicrobium* sp. Root495

wherein a styrene monooxygenase is located between the CoA-DSR and the transcriptional regulator. The same is true for *Nocardioides* sp. Root240 except for a 13983-bp insertion right after the styrene monooxygenase gene. Interestingly, the closest characterized homologs of GCWB2_24025 and GCWB2_24020 can be found in *Rhodococcus* sp. AD45 (WP_045063294 – 59%; WP_045063292 – 49%) and are known to be a functional part of an isoprene degradation cluster which is located on a megaplasmid (300 kbp) (22). In addition, homologs of other genes from cluster S3 can be found on this plasmid, even in a similar arrangement of parts from this cluster. However, strain AD45 does not encode for a styrene monooxygenase on its genome and on the other hand strain CWB2 is lacking the isoprene monooxygenase. Homologous proteins from cluster S3 were recently found in *Gordonia* sp. i37 next to a homologous to cluster S2 (21). The 13983-bp insertion of *Nocardioides* sp. Root240 comprises a putative mce operon, a cluster of membrane proteins whose specific function is unclear.

The putative styrene degradation cluster is completed by a fourth gene set S4 (*GCWB2_24005* - *GCWB2_23925*) that encodes for proteins which are required for the lower styrene degradation pathway (phenylacetic acid catabolism). The proposed pathway of strain CWB2 is displayed in Figure 3b. Besides some regulatory elements and a partial gene (*GCWB2_24000*), this cluster is homolog to that of *Rhodococcus opacus* 1CP and can also be found in *Gordonia soli* NBRC 108243 as well as *Gordonia* sp. i37 (contig69). The AraC-like transcriptional regulator (GCWB2_24005) shows homology to regulators of strain 1CP, that are located bevor the SMO and behind the PAA degradation cluster (ANS32446 – 46%; WP_061046101 – 41%). However, in contrast to strain CWB2 the upper and lower styrene degradation pathways are not associated in this strain. Here the genes for the conversion of styrene to phenylacetic acid are located on a plasmid pR1CP1 (NZ_CP009112),

whereas the subsequent metabolization is encoded on the chromosome (NZ_CP009111). The second transcriptional regulator (GCWB2_23980) belongs to the TetR-family. Cluster S4 is terminated by a phenylacetaldehyde dehydrogenase (GCWB2_23925) that is highly similar to StyD from *Rhodococcus* sp. ST-5 (BAL04135 – 76%). So far, a comparable genetic environment of styrene monooxygenases can only be found in *Aeromicrobium* sp. Root495 and in five strains of *Nocardioides* sp. (Root79, Root190, Root240, Root614, Root682). All of them were isolated from *Arabidopsis* root microbiota (23).

As already mentioned, the whole cluster embeds 3 HTH-type regulators, which are known to respond to aromatic compounds (24). They are not similar to the regulation machinery as described for pseudomonads (3).

Besides this, the genome of strain CWB2 was examined for other genes and clusters that might enable degradation of styrene or metabolites. As no styrene oxide isomerase gene (*styC*) is located on the genome of strain CWB2, it might be possible that this degradation step is bypassed by a styrene oxide reductase (SOR) and a phenylacetaldehyde reductase (PAR). So far, there is no enzyme characterized that has SOR activity and thus no comparison with strain CWB2 on DNA level is possible. However, two putative ORFs (GCWB2_12345 – 70%; GCWB2_18410 – 35%) show similarity to the PAR of *Rhodococcus* sp. ST-10 (BAD51480). Interestingly, the latter one is part of a cluster with 8 ORFs (GCWB2_18380 - GCWB2_18415) that is homolog to one in *Gordonia* sp. TY-5 (BAD03956 - BAD03963; 87 - 96%) (25). It comprises a chaperonin, a putative alcohol dehydrogenase, two hypothetical proteins and a putative propane monooxygenase. The monooxygenase has also resemblance with a propene monooxygenase from *Mycobacterium* sp. M156 (28 - 38%) (26) but also a methane monooxygenase from *Methylococcus capsulatus* Bath (29 - 34%)

208 (27). These binuclear iron monooxygenases are able to epoxidize styrene.
209 Homologous clusters can be found in several actinobacteria (28–30), for instance in
210 *R. opacus* 1CP and *Gordonia* sp. i37 (21). The other putative PAR is not part of a
211 cluster. In addition, several cytochrome P450 monooxygenases can be found on the
212 CWB2 genome, which might also be able to perform the epoxidation of styrene.

213 **Transcriptome and proteome analysis of the styrene degrader CWB2.** The
214 transcriptome and proteome of strain CWB2 was analysed to reveal the global profile
215 of genes and proteins that are involved in styrene metabolism. Therefore, fructose-
216 grown cultures served as reference condition. The transcriptome output is
217 summarized in Table S4.

218 If assuming a threshold of ≥ 1.5 (M-value), then 2.5% of the genes of strain
219 CWB2 are overexpressed under styrene exposure and 30% of these are located on
220 the plasmid (Fig. S5). It is known, that the transcriptome as the total amount of
221 mRNA does not necessarily reflect the total amount of proteins abundance in the cell.
222 However, we were able to identify 3691 proteins in the proteome of strain CWB2. If
223 assuming a threshold of 1.5 (log2 ratio), then 7% of the proteins where highly
224 abundant, when strain CWB2 was grown on styrene (Fig. S6). The gene cluster,
225 which is framed by the styrene monooxygenase and the phenylacetaldehyde
226 dehydrogenase, is highly upregulated on transcriptome (increased on average 7-fold)
227 as well as proteome level (increased on average 6.6-fold) (Table 2 and Dataset S1).

228 **Validation of enzymatic activity of selected members of the styrene**
229 **degradation pathway.** After analysis of the genome, transcriptome and proteome of
230 strain CWB2, we screened for enzyme activities that enable styrene degradation on
231 different pathways. For that, crude extract from styrene grown biomass was
232 prepared, proteins were separated and enriched by different chromatography

methods. The activities were measured directly or indirectly on a spectrophotometer or by quantification of the products on the reverse phase HPLC (RP-HPLC), respectively (Table S5). It was possible to detect SMO activity in the crude extract and to enrich the enzyme 36-fold to an activity of 6.82 mU mg^{-1}. Due to the missing SOI, it was proposed that the conversion of styrene oxide is bypassed by the activity of a SOR, which produces 2-phenylethanol. This is supposed to be converted to phenylacetaldehyde by a PAR. Only minor activity of a PAR with 2-phenylethanol was detected in crude extract. Higher activities were determined in crude extracts, when styrene oxide was applied as substrate. However, this might be due to activity of a GST, while residual glutathione (GSH) is present in the crude extract of strain CWB2. To further prove this assumption, crude extract was assayed for GST activity after supply of additional GSH. Thereby, a GST activity of 44.23 U mg^{-1} was reached for the conversion of styrene oxide (Fig. 2).

Further, crude extracts were assayed for vinylcatechol-2,3-dioxygenase and *cis,cis*-muconate cycloisomerase (MCI) to exclude other degradation pathways. However, there was no detectable activity for one of these enzymes.

Two putative SMOs of strain CWB2 were cloned and expressed for initial characterization. Of the two putative SMOs, only one was expressed and synthesised in an active form. It is part of the styrene degradation cluster (S1; GCWB2_24100) and produces *(S)*-styrene oxide with a specific activity of 0.42 ± 0.02 U mg^{-1}. The SMO can be classified as E1-type SMO (Fig. S2). PADs are aldehyde dehydrogenases that catalyze the formation of the central intermediate phenylacetic acid. Two aldehyde dehydrogenases of strain CWB2 were recombinantly expressed in *E. coli*. Aldh1 which originates from the isoprene degradation cluster (S3) catalyzes the conversion of phenylacetaldehyde with an activity of 0.29 ± 0.01 U mg^{-1}. StyD,

which is encoded in cluster S4 is 10-times slower and has an activity of 0.026 ± 0.001 U mg^{-1}.

DISCUSSION

Adaption of *G. rubripertincta* CWB2 to styrene exposure. Only few reports exist for *Gordonia* considering the metabolization of styrene (18, 31). Further, the limited amount of SMOs that are encoded on genomes of this genus indicate that styrene degradation is no common feature. *Gordonia rubripertincta* CWB2 is able to withstand and degrade high amounts of styrene (520 g m^{-3} in 21 h), even compared to other efficient styrene degraders (32, 33). Some bacteria produce surfactants, when they are exposed to hydrophobic substrates, to increase their accessibility (34–36). However, we found no indication that strain CWB2 exports biosurfactants into the media but it seems to have a hydrophobic cell surface, which improves substrate uptake. This is supported by a tendency to form agglomerates during growth in liquid media.

There is no complete prokaryotic transcriptome under styrene exposure available yet. So far, studies focused on the transcriptional regulation of styrene degradation and a small number of target genes, solely with respect to *Pseudomonas* strains (37–44). A proteome of *R. jostii* RHA1, which employs an unspecific styrene degradation route, is available (45). So far, only one system level proteome analysis for styrene degradation in *P. putida* CA-3 exists (46). It was the first time where all of the respective enzymes of the upper and lower degradation pathway were detected, when a strain was grown on styrene (46).

Omic analysis of strain CWB2 in this study outlines the biological background for its adaption to styrene as source of carbon and energy. This was found to be totally

different to so far characterized styrene degraders. Initially styrene has to be imported into the cell. The only specific styrene transporter StyE was found in pseudomonads (47). However, the *styE* gene is not encoded in most other styrene degraders and thus, other transport mechanisms as well as diffusion have to be considered (3, 46). Cluster S2 of strain CWB2 contains several membrane proteins that are highly upregulated and the same cluster is also present in the styrene degrader *R. opacus* 1CP (Fig. 1). Thus, it is likely that these proteins might also be involved in substrate transport or cell membrane adaption. Interestingly, *Gordonia* sp. i37 owns a similar cluster in proximity of an isoprene degradation cluster (21). However, there are no characterized homologs available in the database and thus the specific function of these proteins remains unclear.

Strain CWB2 merged clusters to form a hybrid that enables styrene degradation. The genetic organisation of the putative styrene degradation cluster compared to other clusters with homolog proteins can be found in Figure 1. The "classical" styrene degradation cluster of *Pseudomonas* sp. Y2 differs to *Rhodococcus* clusters as well as the recently reported cluster of *S. fribergensis* Kp5.2 (17, 38, 48). Thus, it is obvious that the arrangement and regulation is variable among different organisms. The styrene degradation cluster of strain CWB2 is highly upregulated on mRNA and protein level, when strain CWB2 grows on styrene (Table 2 and Dataset S1). In *Pseudomonas* putida CA-3 the SMO and PAD were the most abundant proteins (46). In strain CWB2 they are also highly upregulated but in a comparable range to the rest of the genes and proteins of this cluster. It can be seen that the transcriptional regulators (GCWB2_24035; GCWB2_23980) are less expressed and synthesized. It is also obvious that regulation of gene expression differs in strain CWB2 as no StyR/StyS homolog is associated to this cluster.

However, further studies with different inducers are necessary to clarify the regulation.

There is no evidence that strain CWB2 performs direct ring cleavage of styrene or activation by an epoxide hydrolase as the respective parts of these pathways are not present on the genome or upregulated in the transcriptome or proteome, when cultivated on styrene (supplemental material). In contrast, initial epoxidation of styrene was found to be catalyzed by a SMO. Enzyme activity was detected in crude extracts of styrene-grown cells and the SMO was successfully enriched by ion-exchange chromatography and hydrophobic interaction chromatography (Table S5). The SMO (GCWB2_24100; ASR05591) was recombinantly expressed and purified. The specific epoxidation activity is about 0.4 U mg^{-1} and thus higher than for most other characterized SMOs (48–50). However, epoxidation of styrene is usually the rate-limiting step due to the relative low activity of the SMOs (51).

The SMO is part of cluster S1, which is highly similar to the partial styrene degradation cluster of *Rhodococcus* sp. ST-10. Toda and co-workers proposed chemical conversion of styrene oxide or the cooperation of a styrene oxide reductase (SOR) and phenylacetaldehyde reductase (PAR) (12, 13) as no SOI is present in this strain. However, previous as well as this study indicate that this is rather unlikely, as we detected only minor SOR and PAR activity in the crude extract of strain CWB2. Both assumptions would not explain fast degradation of styrene as found in these strains (3, 52, 53). However, strain ST-10 accumulated the epoxide when incubated with styrene and thus it remains to be shown if the rest of the genes are also homolog to the styrene degradation cluster in strain CWB2.

To circumvent this missing link of enzymatic styrene oxide isomerization, strain CWB2 seems to have incorporated a cluster (S3), which is very similar to ones from

Aeromicrobium sp. Root495 and *Nocarioides* sp. Root240. Interestingly, both were isolated at the same site (23) and both clusters are as well closely located to a styrene monooxygenase in these strains. The genes of cluster S3 may originate from an isoprene degradation cluster as found on a megaplasmid in *Rhodococcus* sp. AD45 (AJ249207) but also in *Gordonia* sp. i37 (21, 54). Actinobacteria from the genera *Mycobacterium*, *Rhodococcus* and *Gordonia* were constantly detected in different environments as isoprene degraders (21, 54, 55). *Rhodococcus* sp. AD45 initially epoxidizes isoprene by the activity of an isoprene monooxygenase. Then it uses a glutathione *S*-transferase to convert the epoxide to a glutathione-alcohol adduct, which is further metabolized by a dehydrogenase to form an aldehyde and subsequently an acid (22, 54, 56–59). Remarkably, strain AD45 is also able to metabolize styrene but has no SMO (56). Derived from these observations, it might be possible that styrene is also channelled through the isoprene degradation pathway in *G. rubripertincta* CWB2. Further, strain CWB2 owns genes that are necessary for glutathione synthesis and reduction in cluster S3 (60). Interestingly, strain CWB2 does not possess an isoprene monooxygenase and has no ability to catabolize isoprene (Table 1).

Styrene oxide is channelled into a novel glutathione dependent degradation pathway. To proof, whether glutathione dependent metabolization occurs, we assayed crude extract from styrene grown cells for GST activity with *(S)*-styrene oxide as substrate. We found that the epoxide was degraded fast with an activity of 44 U $mg_{crude\ extract}^{-1}$ (Fig. 2). Only minor activity was detected when no reduced glutathione was added to the reaction.

Therefore, we propose a novel degradation pathway for styrene via initial epoxidation by a SMO to *(S)*-styrene oxide and addition of glutathione by the GST

358 StyI (Fig. 3a). The resulting *(S)*-(1-Phenyl-2-hydroxyethyl) glutathione (CAS: 64186-
359 97-6) will be further converted by the dehydrogenase StyH to *(S)*-(1-Phenyl-2-
360 acetaldehyde) glutathione and *(S)*-(1-Phenyl-2-acetic acid) glutathione. It might be
361 possible that the phenylacetaldehyde dehydrogenase (PAD) and/or the aldehyde
362 dehydrogenase (Adh1) are also involved in this step as both showed activity with
363 phenylacetaldehyde (61). As the glutathione adduct is not easily accessible it has to
364 be verified if the Adh1 and the PAD can also catalyze this reaction. It was shown that
365 the aldehyde dehydrogenase of cluster S3 are induced in strain AD45 but no specific
366 role had been ascribed (22). Subsequently the glutathione is removed from the
367 adduct what might occur by the activity of StyJ and StyG (58, 62, 63). The product of
368 this process will be phenylacetic acid or phenylacetyl-CoA, which will be degraded
369 via several enzymes from cluster S4 to yield acetyl-CoA and succinyl-CoA (Fig. 3b).
370 We suppose that the 2-phenylethanol and phenylacetaldehyde, that can be detected
371 during growth, results from side-product formation of this novel pathway due to
372 instability of the glutathione adducts or enzymatic removal of glutathione in an earlier
373 step (Fig. 3a).

374 It should be mentioned that it is unusual for actinobacteria to produce glutathione,
375 as mycothiol is the dominant thiol in these organisms (64–66). However, it was
376 reported that strain AD45 additionally produces substantial amounts of glutathione
377 and it was suggested that this ability was gained by horizontal gene transfer of
378 isoprene degradation genes (54, 56, 58, 65). It is likely that the same is true for strain
379 CWB2 due to the plasmid uptake. This is supported by the finding that the GC
380 content of the plasmid and the styrene degradation cluster is much lower compared
381 to the whole genome. The GC content of that cluster S3 is close to that of strain
382 AD45 (61.7%; (22). Recently, genes of cluster S3 were found in *Gordonia* sp. i37
383 (21). Further, strain CWB2 as well as strain 1CP encode for several mobile elements

384 in direct neighbourhood of the styrene degradation cluster on their plasmid what
385 suggests horizontal gene transfer. In addition, the cluster S4 is highly similar that that
386 of *R. opacus* 1CP and strain RHA1 and degradation of PAA likely takes place in the
387 same way (67, 68) (Fig. 3b).

388

389 **CONCLUSION**

390 Omic analyses imply that strain CWB2 incorporated a plasmid which contains an
391 assembly of different gene clusters and forms a “hybrid” that enables to metabolize
392 styrene and analogous compounds. Our study illustrates the possibilities of horizontal
393 gene transfer for Gram-positive bacteria and an ongoing adaptation to glutathione as
394 cofactor in actinobacteria. This adaption is coupled with a high biotechnological
395 potential of this organism, as *G. rubripertincta* CWB2 can produce ibuprofen, which is
396 not possible through the classical styrene degradation pathway (17, 18). The
397 involved SMO shows higher activities than reported for other SMOs so far. This might
398 be interesting as these enzymes are known to catalyze a variety of valuable reactions
399 (3). Further, bacterial GST are known to be involved in degradation of (halogenated)
400 xenobiotics and other chemical transformations and therefore the GST of strain
401 CWB2 might open a new field of possible biochemical reactions to this class of
402 enzymes (63, 69, 70).

403 **MATERIALS AND METHODS**

404 **Isolation and cultivation of styrene-degrading strains.** Styrene degrading
405 bacteria were isolated from (contaminated) soil. A small amount of the soil was
406 transferred into a 1-l Erlenmeyer flask and suspended in 100 ml water. Portions of 10
407 to 40 µl of styrene were supplied via an evaporation adaptor as sole source of carbon
408 and energy. The growth media was dosed with 0.02 mg ml^{-1} nalidixin acid and 0.075
409 mg ml^{-1} cycloheximide to prevent growth of Gram-negative bacteria or fungi,
410 respectively. 10 ml of the culture was plated on solid mineral medium (MM) (71)
411 without carbon source and incubated at room temperature in a 5-l desiccator under
412 styrene containing atmosphere. The grown colonies were repeatedly transferred on
413 fresh solid mineral media and incubated for 2 - 3 days in the desiccator. The isolates
414 were stored at - 80°C in 40% (v/v) glycerol.

415 Liquid cultures were kept in Erlenmeyer flasks containing mineral media (71). The
416 respective carbon source was added either directly into the media or in case of
417 volatile compounds via an evaporation adapter.

418 **Characterization of *G. rubripertincta* CWB2.** Growth of strain CWB2 in liquid
419 MM was assayed on various substrates (Table S1). Production of surfactants with
420 fructose, hexadecane or styrene as carbon source was examined as published
421 earlier (36, 72). Siderophore production was determined by the CAS-agar plate test
422 (73). Analysis of the mycol- and fatty acid composition was done by the Deutsche
423 Sammlung für Mikroorganismen und Zellkulturen (DSMZ) (Table S2). 16S rRNA
424 analysis and Scanning electron microscopy (SEM) was done as described earlier
425 (18) (Fig. S1 and S3). The *in silico* DNA-DNA-hybridization was performed by the
426 Genome-to-Genome Distance Calculator 2.1 (DSMZ) (Fig. S7). *G. rubripertincta*

CWB2 was assayed for antibiotic resistance on chloramphenicol, ampicillin, tetracycline, nalidixic acid, gentamycin, streptomycin and kanamycin.

DNA extraction and genome sequencing, annotation and bioinformatic analysis. A 50-ml culture of *G. rubripertincta* CWB2 was grown on fructose in mineral media. Cells were harvested at an OD_{600} of 0.6 by centrifugation (5 000 x g; 15 min), washed once with 100 mM phosphate buffer (pH 7.5) and centrifuged again. The cell Pellet was resuspended in 2.7 ml buffer (10 Tris-HCl, 10% sucrose, 30 mg lysozyme; pH 7.8) and incubated for 1.5 h at 37°C. After centrifugation the supernatant was discarded and the pellet was resuspended in 2.8 ml TE-buffer 10.1 (10 mM Tris, 1 mM EDTA; pH 8) with 100 µg ml^{-1} proteinase K and 150 µl SDS (10%) and incubated for 2 h at 37°C. Chromosomal DNA was extracted successively with 3 to 5 ml phenol (equilibrated; 2 times), phenol:chloroform:isoamyl alcohol (25:24:1) and chloroform:isoamyl alcohol (24:1; 2 times). Each extraction was followed by a centrifugation (20 000 x g; 10 min) and separation of the aqueous phase into a new tube. Afterwards, RNA was digested by adding 100 µg ml^{-1} RNase A at 37°C for 10 min. The DNA was precipitated on ice by the addition of 1/10 volume of 3 M sodium acetate (pH 5.2) and 3 volumes of 100% ethanol. The precipitate was centrifuged at 4°C, resuspended in 70% ice-cold ethanol and centrifuged again. The supernatant was discarded and the pellet was dried for 10 min in a SpeedVac vacuum concentrator. The pellet was dissolved in TE-buffer 10.1 for storage at 4°C and purity was controlled by agarose-gel electrophoresis and on the Nanodrop.

To obtain the complete genome sequence, two sequencing libraries were prepared, a TruSeq PCR-free whole genome shotgun library and a 8k Nextera MatePair libary (Illumina Inc, Netherlands). Both libraries were sequenced on an Illumina MiSeq desktop sequencer with 2x 300 bp. The obtained reads were

assembled using the Newbler (v2.8) *de novo* assembler (Roche). The initial assembly consisted of just one scaffold of 90 contigs, with 120 contigs larger than 500 bp in total. Manual inspection and assembly was performed using CONSED (74, 75), which revealed a misassembly: 3 contigs representing a 105 kbp plasmid, henceforth called pGCWB2, were wrongly "attached" to the scaffold representing the chromosome. The sequence of both replicons could be completely established. The sequences for both replicons were annotated using PROKKA (76), see Table S3 for details. The annotated replicons were submitted to GenBank, the accession numbers are CP022580 (chromosome) and CP022581 (pGCWB2)

Additional functional annotation of proteins was done by using the BLASTP algorithm (20) on the non-redundant protein database or the UniProtKB database (NCBI) (date of search: 01.09.2017). Membrane association of proteins was verified by prediction on the TMHMM server (77). Island viewer 4 (78) was applied to detect genomic islands and foreign genes on the genome of strain CWB2 (Fig. S4).

RNA extraction and transcriptome sequencing. A pre-culture of *G. rubripertincta* CWB2 was grown at 30°C in minimal media with fructose or styrene as sole source of carbon, respectively. After 5 days of cultivation the culture was diluted 1/10 in fresh media and incubated for 24 h with the respective substrate in a set of four Erlenmeyer flasks. Prior harvesting the cells, 10% of an ice-cold STOP-solution (10% buffered phenol in ethanol) was added to the culture followed by centrifugation at 11 000 x g for 5 min at 4°C. The supernatant was discarded and the pellet was stored until RNA isolation at - 80°C. To break up the cells, 150 µl of a 5 mg ml^{-1} lysozyme solution were added to the pellet, mixed and incubated at room temperature for 5 min. 450 µl of buffer RLT (Qiagen) and 50 mg of (0.1 mm) glass beads were added to resuspend and break the cells by repeated vortexing at 4°C.

The suspension was applied to QIAshredder column for homogenization and to remove particles from the sample. Extraction of total RNA Extraction was done by applying the RNeasy Mini Kit including on-column DNA digestion (Qiagen). Isolated RNA was stored at - 80°C and quality was controlled on the 2100 Bioanalyzer using the RNA 6000 Nano Kit (Agilent).

RNA quality and quantity was again checked by an Agilent 2100 Bioanalyzer run (Agilent Technologies, Böblingen, Germany) and Trinean Xpose sytem (Gentbrugge, Belgium) prior and after rRNA depletion by Ribo-Zero rRNA Removal Kit (Bacteria) (Illumina, San Diego, CA, USA). TruSeq Stranded mRNA Library Prep Kit from Illumina, (San Diego, CA, USA) was used to prepare the cDNA libraries to analyze the whole transcriptome. The resulting cDNAs were then sequenced paired end on an Illumina MiSeq and HiSeq 1500 system (San Diego, CA, USA) using 2 x 75 nt read length. The raw sequencing read files are available in the ArrayExpress database (www.ebi.ac.uk/arrayexpress) under accession number: E-MTAB-6012. Reads were mapped on the reference *G. rubripertincta CWB2* (CP022580, CP022581) with Bowtie2 (79) using standard settings. ReadXplorer 2.2.0 (80) was used for visualization of short read alignments and data analysis. Differential gene expression analysis was performed based on normalized read count using TPM values (Transcripts Per Million) of CDS calculated by ReadXplorer 2.2.0. The signal intensity value (a-value) was calculated by 0.5*(log2 TPM condition A + log2 TPM condition B) of each CDS and the signal intensity ratio (m-value) by the difference of (log2) TPM. CDS with m-values of higher/equal than +1.5 or lower/equal than −1.5 were considered to be differentially transcribed.

Preparation of protein samples and identification by LC-ESI-MS/MS mass spectrometry. *G. rubripertincta* CWB2 was grown the same way as for RNA

extraction in a set of four samples per carbon source. After cultivation, two samples were pooled and centrifuged at 5 000 x g for 30 min at 4°C and resuspended in 2.5 ml 50 mM PP, pH 7.26. The cells were disrupted by sonication on ice (10 cycles, 1.5 min; power: 70%; BANDELIN Sonoplus Homogenisator HD2070) after adding 40 U DNAseI and 1 mg ml^{-1} lysozyme. The suspension was centrifugated at 50 000 x g for 1 h at 4°C to separate soluble from insoluble matter. The proteins were separated by size using discontinuous sodium dodecyl sulfate-polyacrylamide gel electrophoresis (SDS-PAGE) with 50 µg of each sample per lane. Lanes were cut into 8 slices and de-stained, alkylated and digested with trypsin as previously described (81, 82). Peptides were extracted from the gel pieces with acetonitrile, loaded onto STAGE tips for storage, and eluted from the tips shortly before MS analysis (83).

By using an EASY- nLC 1000 (Thermo Scientific) LC system, peptides were separated at a flow rate of 400 nl/min on a 18 cm self-packed column (75 µm ID, 1.9 µm Reprosil-Pur 120 C-18AQ beads, Dr Maisch Germany) housed in a custom-built column oven (84) at 45°C. Peptides were separated using gradient of buffers A (0.1% formic acid) and B (80% acetonitrile, 0.1% formic acid) from 1% to 60% B. The column was interfaced with a Nanospray Flex Ion Source (Thermo Scientific) to a Q-Exactive HF mass spectrometer (Thermo Scientific). MS instrument settings were: 1.5 kV spray voltage, Full MS at 60K resolution, AGC target 3e6, range of 300 - 1750 m/z, max injection time 20 ms; Top 15 MS/MS at 15K resolution, AGC target 1e5, max injection time 25 ms, isolation width 2.2 m/z, charge exclusion +1 and unassigned, peptide match preferred, exclude isotope on, dynamic exclusion for 20s.

Mass spectra were recorded with Xcalibur software 3.1.66.10 (Thermo Scientific). Using a custom database containing 4831 predicted protein sequences, proteins were identified with Andromeda and quantified with the LFQ algorithm embedded in

MaxQuant version 1.5.3.17 (85). The following parameters were used: main search max. peptide mass error of 4.5 ppm, tryptic peptides of min. 6 amino acid length with max. two missed cleavages, variable oxidation of methionine, protein N-terminal acetylation, fixed cysteine carbamidomethylation, LFQ min. ratio count of 2, matching between runs enabled, PSM and (Razor) protein FDR of 0.01, advanced ratio estimation and second peptides enabled. Proteins with a log2 ratio of higher/equal than +1.5 or lower/equal than −1.5 were considered to be differentially synthesized.

Cloning, expression and purification of recombinant styAs, styD and aldh1. The *styA* (*GCWB2_24100*, *GCWB2_21620*), *styD* (*GCWB2_23925*) and *aldh1* (*GCWB2_24010*) genes were purchased from Eurofins MWG (Ebersberg) in a pEX-K2 vector system allowing for kanamycin resistance selection. The DNA sequences were optimized for the codon usage and GC content of *Acinetobacter baylyi* ADP1 with the OPTIMIZER tool (48, 86). 5'-NdeI and 3'-NotI restriction sites were added and used for subcloning into pET16bP to obtain the expression constructs pSGrA1_P01, pSGrA2_P01 and pSGrD1_P01, pSGrD2_P01 from which recombinant proteins can be obtained as His_{10}-tagged proteins. *Escherichia coli* strain DH5α and strain BL21 (DE3) pLysS were cultivated for cloning and expression purposes as described elsewhere (87). Plasmids are listed in Table 3.

Expression of StyA's took place in a 3-l biofermenter. *E. coli* BL21 strains with the respective plasmids were cultivated in LB media (100 µg ml^{-1} ampicillin and 50 µg ml^{-1} chloramphenicol) at 30°C until an OD_{600} of 0.4 was reached. The batch was subsequently cooled to 20°C. Expression was induced at an OD_{600} of 0.6 by adding 0.1 mM of IPTG (isopropyl-β-$_D$-thiogalactopyranoside) to the culture and grown for 20 h at 20°C (120 rpm). Cells were harvested by centrifugation (5 000 x g, 30 min, 4°C), resuspended in 10 mM Tris-HCl buffer (pH 7.5) and stored at - 80°C. Formation of

552 the blue dye indigo is observable if active SMOs are produced during expression in
553 LB media (88). As this was not the case for expression of *GCWB2_21620* we
554 assumed that the protein is not synthesized or active.

555 For purification of StyA, crude extracts were prepared from freshly thawed
556 biomass by disruption in a precooled French Pressure cell, followed by centrifugation
557 to remove cell debris (50 000 x g, 2 h, 4°C). The supernatants were applied to a 1-ml
558 HisTrap FF column. The column was washed with 10 CV of binding buffer (10 mM
559 Tris-HCl, 0.5 M NaCl, 25 mM imidazole, pH 7.5) to remove nonspecific bound
560 proteins. Enzymes were eluted with a linear imidazole gradient up to 500 mM over 30
561 CV. Fractions with respective enzyme activity (see 2.6.) were pooled and
562 concentrated using Sartorius Vivaspin 20 filters (5 000 MWCO) at 4°C. The
563 concentrates were passed through a 10-ml Econo-Pac 10DG desalting gravity-flow
564 column (Bio-Rad) to remove remaining imidazole and sodium chloride. Protein
565 obtained was kept in storage buffer (10 mM Tris-HCl, 50% [v/v] glycerol, pH 7.5) at -
566 20°C. Expression of *GCWB2_21620* did not yield active protein as already
567 mentioned. Preparation of StyD and Aldh1 was done according to Zimmerling *et al.*
568 2017 (61).

569 **Purification of wild-type proteins.** All following purification steps were
570 performed on an ÄKTA fast-performance liquid chromatographer (GE Healthcare).
571 Selected wild-type enzymes were enriched from crude extract by ion-exchange
572 chromatography. Therefore, strain CWB2 was cultivated on styrene and soluble
573 crude extract was prepared as described above. The supernatant was loaded with
574 buffer A (20 mM Tris-HCl; pH 7.5) on a MonoQ HR 5/5 column (GE Healthcare) at a
575 flow rate of 1 ml min^{-1}. Nonspecific bound proteins were removed by washing with 5
576 column volumes (CV) of buffer A. Elution of proteins was done over 25 CV with a

linear gradient of buffer B (20 mM Tris-HCl, 1 M NaCl; pH 7.5). Fractions of 1 ml were collected and tested on the respective enzyme activity. A second purification step was applied for some enzymes by using hydrophobic interaction chromatography. Therefore, the fractions that showed the respective enzyme activity were pooled and $(NH_4)_2SO_4$ was added to a final concentration of 460 mM. The sample was loaded with buffer C (20 mM Tris-HCl, 0.8 M $(NH_4)_2SO_4$; pH 7.5) on a 1-ml Phenyl HP HiTrap column (GE Healthcare) at a flow rate of 1 ml min^{-1}. Nonspecific bound proteins were removed by washing with 5 column volumes (CV) of buffer A. Elution of proteins was done over 25 CV with a linear gradient of buffer A (20 mM Tris-HCl; pH 7.5). Fractions of 1 ml were tested on enzyme activity.

For VC12DO gel filtration was done after hydrophobic interaction chromatography. Therefore, the fraction containing VC12DO activity were pooled and applied with buffer D (25 mM Tris-HCl, 0.5 M NaCl; pH 7.5) to a Superdex 200 HR 10/30 column at a flow rate of 0.4 ml min^{-1}. Fractions of 1 ml were tested for VC12DO activity.

Recombinant and wild-type proteins were subjected to discontinuous sodium dodecyl sulfate-polyacrylamide gel electrophoresis (SDS-PAGE) (87) in order to determine purity and subunit molecular size.

Enzyme assays. Crude extracts, enriched or purified protein preparations from *G. rubripertincta* CWB2 were assayed for enzyme activities that are representative for known degradation pathways of styrene.

Wild-type catechol 1,2-dioxygenase, catechol 2,3-dioxygenase and *cis,cis*-muconate cycloisomerase activity was measured spectrophotometrically (Cary 50, Varian) by following the product formation or substrate depletion according to Warhurst *et al.* 1994 (89) using catechol, protocatechuate and *cis,cis*-muconate as

602 substrates, respectively.

603 Styrene monooxygenase (SMO) activity of wild-type and recombinant enzyme
604 preparations with styrene were measured by quantification of the reaction product
605 styrene oxide on a RP-HPLC system as described previously (90).

606 Styrene oxide reductase (SOR) and phenylacetaldehyde reductase (PAR) wild-
607 type activity with styrene oxide and 2-phenylethanol was determined by quantification
608 of the reaction products phenylacetaldehyde or 2-phenylethanol on a RP-HPLC
609 system following the protocol as described previously for the styrene oxide isomerase
610 (SOI) (17, 18).

611 Wild-type phenylacetaldehyde dehydrogenase (PAD) and wild-type PAR activity
612 was assayed indirectly on a spectrophotometer (Cary 50, Varian) by following the
613 reduction of NAD^+ to NADH at 340 nm ($\varepsilon 340\ nm = 6.22\ mM^{-1}\ cm^{-1}$) (91). The 1 ml
614 assay mixture contained 0.5 mM phenylacetaldehyde or 2-phenylethanol in 10 mM
615 Tris-HCl (pH 7.5), 1 mM NAD^+ and 50 µl protein containing sample, respectively.
616 Recombinant PAD activity was assayed according to (61).

617 GST wild-type activity was assayed in soluble crude extract by following the *(S)*-
618 styrene oxide consumption over time. Therefore, *G. rubripertincta* CWB2 was grown
619 on MM with styrene as sole source of carbon. A 100 ml pre-culture was prepared and
620 used to inoculate the main culture 1:50 in 500 ml fresh MM. The main culture was
621 incubated at 30°C for 5 days by adding 20 to 80 µl portions styrene via gas-phase.
622 Cells were harvested by centrifugation at 5 000 x g for 20 min at 4°C. The
623 supernatant was discarded and the pellet was resuspended and washed 2 times in
624 10 ml 20 mM PP (pH 8). The cells were disrupted by sonication on ice (10 cycles,
625 1 min; power: 70%; BANDELIN Sonoplus Homogenisator HD2070) after adding 40 U
626 DNAseI and 1 mg ml^{-1} lysozyme. Soluble crude extracts were obtained by

627 centrifugation at 50 000 x g at 4°C for 1 h and separation from the insoluble matter.
628 The reaction mix (600 µl) contained 20 mM PP (pH 8), 4 mM *(S)*-styrene oxide, 5 mM
629 GSH and an appropriate amount of soluble crude extract. Blank measurements were
630 carried out by omitting either GSH or enzyme preparation. Samples were tempered
631 for 10 min at 30°C and the reaction was initiated by the addition of the substrate *(S)*-
632 styrene oxide. 25 µl samples were quenched at certain time points in 50 µl ice cold
633 acetonitrile:methanol (1:1) and centrifuged at 16 000 x g for 10 min at 4°C to remove
634 precipitates. Supernatants were applied to RP-HPLC by injection of 10 µl samples.
635 All measurements were done in triplicates. Enzyme activities are given in 1 U mg^{-1}
636 representing the conversion µmol substrate per min per mg protein.

637 All RP-HPLC measurements were done with a Eurospher C_{18} column (125 mm
638 length by 4 mm i.d., 5 µm particle size, 100 Å pore size; Knauer, Germany). The
639 protein content was determined by means of the Bradford method (92), using
640 BradfordUltra reagent (Expedeon) and bovine serum albumin (Sigma) as reference
641 protein.

642 **Accession numbers.** Genome and assembly of *Gordonia rubripertincta* CWB2 is
643 deposited at NCBI (BioProject Accession: PRJNA394617; URL:
644 https://www.ncbi.nlm.nih.gov/bioproject/?term=PRJNA394617) with the chromosome
645 (CP022580) and plasmid (CP022581) sequences.

646 The raw sequencing read files are available in the ArrayExpress database
647 (www.ebi.ac.uk/arrayexpress) under accession number: E-MTAB-6012.

648 Newly characterized recombinant proteins in this study are StyA (ASR05591;
649 https://www.ncbi.nlm.nih.gov/protein/ASR05591), StyD (ASR05556;
650 https://www.ncbi.nlm.nih.gov/protein/ASR05556), Aldh1 (ASR05573;

651 https://www.ncbi.nlm.nih.gov/protein/ASR05573) and the monooxygenase
652 (ASR05096; https://www.ncbi.nlm.nih.gov/protein/ASR05096).

653

654 **ACKNOWLEDGEMENTS**

655 We appreciate the funding of this project by the Deutsche Bundesstiftung Umwelt
656 (DBU), the European Social Fund and the Saxonian Government (GETGEOWEB:
657 100101363).

658 We hereby declare no conflicting interests among all of us the co-authors.

659

660

661 **SUPPLEMENTAL MATERIAL**

662 Supplemental material is available at AEM’s website.

663

664

REFERENCES

1. Bond JA. 1989. Review of the toxicology of styrene. Crit Rev Toxicol 19:227–249.
2. Gibbs BF, Mulligan CN. 1997. Styrene toxicity: an ecotoxicological assessment. Ecotoxicol Environ Saf 38:181–194.
3. Tischler D. 2015. Microbial styrene degradation. Springer Verlag.
4. van Agteren MH, Keuning S, Janssen DB, Janssen JP, Oosterhaven J. 2010. Handbook on biodegradation and biological treatment of hazardous organic compounds. Environment and Chemistry, v. 2. Springer Netherlands, Dordrecht.
5. Tischler D, Kaschabek SR. 2012. Microbial styrene degradation. From basics to biotechnology, 67–99. *In* Singh SN (ed), Microbial degradation of xenobiotics. Springer-Verlag, Berlin Heidelberg.
6. Mooney A, Ward PG, O'Connor KE. 2006. Microbial degradation of styrene: biochemistry, molecular genetics, and perspectives for biotechnological applications. Appl Microbiol Biotechnol 72:1–10.
7. Crabo AG, Singh B, Nguyen T, Emami S, Gassner GT, Sazinsky MH. 2017. Structure and biochemistry of phenylacetaldehyde dehydrogenase from the *Pseudomonas putida* S12 styrene catabolic pathway. Arch Biochem Biophys 616:47–58.
8. Teufel R, Mascaraque V, Ismail W, Voss M, Perera J, Eisenreich W, Haehnel W, Fuchs G. 2010. Bacterial phenylalanine and phenylacetate catabolic pathway revealed. Proc Natl Acad Sci USA 107:14390–14395.
9. Grishin AM, Cygler M. 2015. Structural organization of enzymes of the phenylacetate catabolic hybrid pathway. Biology (Basel) 4:424–442.
10. Itoh N, Yoshida K, Okada K. 1996. Isolation and identification of styrene-degrading *Corynebacterium* strains, and their styrene metabolism. Biosci Biotechnol Biochem 60:1826–1830.
11. Itoh N, Hayashi K, Okada K, Ito T, Mizuguchi N. 1997. Characterization of styrene oxide isomerase, a key enzyme of styrene and styrene oxide metabolism in *Corynebacterium* sp.. Biosci Biotechnol Biochem 61:2058–2062.
12. Itoh N, Morihama R, Wang J, Okada K, Mizuguchi N. 1997. Purification and characterization of phenylacetaldehyde reductase from a styrene-assimilating *Corynebacterium* strain, ST-10. Appl Environ Microbiol 63:3783–3788.
13. Toda H, Itoh N. 2012. Isolation and characterization of styrene metabolism genes from styrene-assimilating soil bacteria *Rhodococcus* sp. ST-5 and ST-10. J Biosci Bioeng 113:12–19.
14. Marconi AM, Beltrametti F, Bestetti G, Solinas F, Ruzzi M, Galli E, Zennaro E. 1996. Cloning and characterization of styrene catabolism genes from *Pseudomonas fluorescens* ST. Appl Environ Microbiol 62:121–127.
15. Arenskötter M, Bröker D, Steinbüchel A. 2004. Biology of the metabolically diverse genus *Gordonia*. Appl Environ Microbiol 70:3195–3204.
16. Drzyzga O. 2012. The strengths and weaknesses of *Gordonia*: a review of an emerging genus with increasing biotechnological potential. Crit Rev Microbiol 38:300–316.

17. Oelschlägel M, Zimmerling J, Schlömann M, Tischler D. 2014. Styrene oxide isomerase of *Sphingopyxis* sp. Kp5.2. Microbiology (Reading, Engl.) 160:2481–2491.
18. Oelschlägel M, Kaschabek SR, Zimmerling J, Schlömann M, Tischler D. 2015. Co-metabolic formation of substituted phenylacetic acids by styrene-degrading bacteria. Biotechnol Rep 6:20–26.
19. Esuola CO, Babalola OO, Heine T, Schwabe R, Schlömann M, Tischler D. 2016. Identification and characterization of a FAD-dependent putrescine N-hydroxylase (GorA) from *Gordonia rubripertincta* CWB2. J Mol Catal B: Enzym 134:378–389.
20. Altschul SF, Gish W, Miller W, Myers EW, Lipman DJ. 1990. Basic local alignment search tool. J Mol Biol 215:403–410.
21. Johnston A, Crombie AT, El Khawand M, Sims L, Whited GM, McGenity TJ, Colin Murrell J. 2017. Identification and characterisation of isoprene-degrading bacteria in an estuarine environment. Environ Microbiol. doi:10.1111/1462-2920.13842.
22. Crombie AT, Khawand ME, Rhodius VA, Fengler KA, Miller MC, Whited GM, McGenity TJ, Murrell JC. 2015. Regulation of plasmid-encoded isoprene metabolism in *Rhodococcus*, a representative of an important link in the global isoprene cycle. Environ Microbiol 17:3314–3329.
23. Bai Y, Müller DB, Srinivas G, Garrido-Oter R, Potthoff E, Rott M, Dombrowski N, Munch PC, Spaepen S, Remus-Emsermann M, Huttel B, McHardy AC, Vorholt JA, Schulze-Lefert P. 2015. Functional overlap of the *Arabidopsis* leaf and root microbiota. Nature 528:364–369.
24. Tropel D, van der Meer JR. 2004. Bacterial transcriptional regulators for degradation pathways of aromatic compounds. Microbiol Mol Biol Rev 68:474-500.
25. Kotani T, Yamamoto T, Yurimoto H, Sakai Y, Kato N. 2003. Propane monooxygenase and NAD^+-dependent secondary alcohol dehydrogenase in propane metabolism by *Gordonia* sp. strain TY-5. J Bacteriol 185:7120–7128.
26. Chan Kwo Chion CK, Askew SE, Leak DJ. 2005. Cloning, expression, and site-directed mutagenesis of the propene monooxygenase genes from *Mycobacterium* sp. strain M156. Appl Environ Microbiol 71:1909–1914.
27. Colby J, Stirling DI, Dalton H. 1977. The soluble methane monooxygenase of *Methylococcus capsulatus* (Bath). Its ability to oxygenate n-alkanes, n-alkenes, ethers, and alicyclic, aromatic and heterocyclic compounds. Biochem J 165:395–402.
28. Furuya T, Hirose S, Osanai H, Semba H, Kino K. 2011. Identification of the monooxygenase gene clusters responsible for the regioselective oxidation of phenol to hydroquinone in mycobacteria. Appl Environ Microbiol 77:1214–1220.
29. Furuya T, Hayashi M, Kino K. 2013. Reconstitution of active mycobacterial binuclear iron monooxygenase complex in *Escherichia coli*. Appl Environ Microbiol 79:6033–6039.
30. Furuya T, Hayashi M, Semba H, Kino K. 2013. The mycobacterial binuclear iron monooxygenases require a specific chaperonin-like protein for functional expression in a heterologous host. FEBS J 280:817–826.

31. Narancic T, Djokic L, Kenny ST, O'Connor KE, Radulovic V, Nikodinovic-Runic J, Vasiljevic B. 2012. Metabolic versatility of Gram-positive microbial isolates from contaminated river sediments. J Hazard Mater 215-216:243–251.
32. Braun-Lüllemann A, Majcherczyk A, Hüttermann A. 1997. Degradation of styrene by white-rot fungi. Appl Microbiol Biotechnol 47:150–155.
33. Gaszczak A, Bartelmus G, Gren I. 2012. Kinetics of styrene biodegradation by *Pseudomonas* sp. E-93486. Appl Microbiol Biotechnol 93:565–573.
34. Bredholt H, Josefsen K, Vatland A, Bruheim P, Eimhjellen K. 1998. Emulsification of crude oil by an alkane-oxidizing *Rhodococcus* species isolated from seawater. Can J Microbiol 44:330–340.
35. Lang S, Philp JC. 1998. Surface-active lipids in rhodococci. Antonie Van Leeuwenhoek 74:59–70.
36. Franzetti A, Bestetti G, Caredda P, La Colla P, Tamburini E. 2008. Surface-active compounds and their role in the access to hydrocarbons in *Gordonia* strains. FEMS Microbiol Ecol 63:238–248.
37. O'Connor K, Buckley CM, Hartmans S, Dobson AD. 1995. Possible regulatory role for nonaromatic carbon sources in styrene degradation by *Pseudomonas putida* CA-3. Appl Environ Microbiol 61:544–548.
38. Velasco A, Alonso S, Garcia JL, Perera J, Diaz E. 1998. Genetic and functional analysis of the styrene catabolic cluster of *Pseudomonas* sp. strain Y2. J Bacteriol 180:1063–1071.
39. Santos PM, Blatny JM, Di Bartolo I, Valla S, Zennaro E. 2000. Physiological analysis of the expression of the styrene degradation gene cluster in *Pseudomonas fluorescens* ST. Appl Environ Microbiol 66:1305–1310. doi:10.1128/AEM.66.4.1305-1310.2000.
40. O'Leary ND, O'Connor KE, Duetz W, Dobson AD. 2001. Transcriptional regulation of styrene degradation in *Pseudomonas putida* CA-3. Microbiology (Reading, Engl.) 147:973–979.
41. Leoni L, Ascenzi P, Bocedi A, Rampioni G, Castellini L, Zennaro E. 2003. Styrene-catabolism regulation in *Pseudomonas fluorescens* ST: phosphorylation of StyR induces dimerization and cooperative DNA-binding. Biochem Biophys Res Commun 303:926–931.
42. Leoni L, Rampioni G, Di Stefano V, Zennaro E. 2005. Dual role of response regulator StyR in styrene catabolism regulation. Appl Environ Microbiol 71:5411–5419.
43. Milani M, Leoni L, Rampioni G, Zennaro E, Ascenzi P, Bolognesi M. 2005. An active-like structure in the unphosphorylated StyR response regulator suggests a phosphorylation-dependent allosteric activation mechanism. Structure 13:1289–1297.
44. del Peso-Santos T, Shingler V, Perera J. 2008. The styrene-responsive StyS/StyR regulation system controls expression of an auxiliary phenylacetyl-coenzyme A ligase. Implications for rapid metabolic coupling of the styrene upper- and lower-degradative pathways. Mol Microbiol 69:317–330.
45. Patrauchan MA, Florizone C, Eapen S, Gomez-Gil L, Sethuraman B, Fukuda M, Davies J, Mohn WW, Eltis LD. 2008. Roles of ring-hydroxylating dioxygenases in

styrene and benzene catabolism in *Rhodococcus jostii* RHA1. J Bacteriol 190:37–47.
46. Nikodinovic-Runic J, Flanagan M, Hume AR, Cagney G, O'Connor KE. 2009. Analysis of the *Pseudomonas putida* CA-3 proteome during growth on styrene under nitrogen-limiting and non-limiting conditions. Microbiology (Reading, Engl.) 155:3348–3361.
47. Mooney A, O'Leary ND, Dobson ADW. 2006. Cloning and functional characterization of the styE gene, involved in styrene transport in *Pseudomonas putida* CA-3. Appl Environ Microbiol 72:1302–1309. doi:10.1128/AEM.72.2.1302-1309.2006.
48. Riedel A, Heine T, Westphal AH, Conrad C, Rathsack P, van Berkel WJH, Tischler D. 2015. Catalytic and hydrodynamic properties of styrene monooxygenases from *Rhodococcus opacus* 1CP are modulated by cofactor binding. AMB Express 5:112.
49. Otto K, Hofstetter K, Röthlisberger M, Witholt B, Schmid A. 2004. Biochemical characterization of StyAB from *Pseudomonas* sp. strain VLB120 as a two-component flavin-diffusible monooxygenase. J Bacteriol 186:5292–5302.
50. Toda H, Imae R, Komio T, Itoh N. 2012. Expression and characterization of styrene monooxygenases of *Rhodococcus* sp. ST-5 and ST-10 for synthesizing enantiopure (*S*)-epoxides. Appl Microbiol Biotechnol 96:407–418.
51. Cheng L, Yin S, Chen M, Sun B, Hao S, Wang C. 2016. Enhancing indigo production by over-expression of the styrene monooxygenase in *Pseudomonas putida*. Curr Microbiol 73:248–254.
52. Han JH, Park MS, Bae JW, Lee EY, Yoon YJ, Lee S-G, Park S. 2006. Production of (*S*)-styrene oxide using styrene oxide isomerase negative mutant of *Pseudomonas putida* SN1. Enzyme Microb Technol 39:1264–1269.
53. Oelschlägel M, Gröning JAD, Tischler D, Kaschabek SR, Schlömann M. 2012. Styrene oxide isomerase of *Rhodococcus opacus* 1CP, a highly stable and considerably active enzyme. Appl Environ Microbiol 78:4330–4337.
54. El Khawand M, Crombie AT, Johnston A, Vavlline DV, McAuliffe JC, Latone JA, Primak YA, Lee S-K, Whited GM, McGenity TJ, Murrell JC. 2016. Isolation of isoprene degrading bacteria from soils, development of *isoA* gene probes and identification of the active isoprene-degrading soil community using DNA-stable isotope probing. Environ Microbiol 18:2743–2753.
55. Alvarez LA, Exton DA, Timmis KN, Suggett DJ, McGenity TJ. 2009. Characterization of marine isoprene-degrading communities. Environ Microbiol 11:3280–3291.
56. van Hylckama VJ, Kingma J, van den Wijngaard, A J, Janssen DB. 1998. A glutathione *S*-transferase with activity towards cis-1,2-dichloroepoxyethane is involved in isoprene utilization by *Rhodococcus* sp. strain AD45. Appl Environ Microbiol 64:2800–2805.
57. van Hylckama VJ, Kingma J, Kruizinga W, Janssen DB. 1999. Purification of a glutathione *S*-transferase and a glutathione conjugate-specific dehydrogenase involved in isoprene metabolism in *Rhodococcus* sp. strain AD45. J Bacteriol 181:2094–2101.

58. van Hylckama VJ, Leemhuis H, Spelberg JHL, Janssen DB, Spelberg JH, van Hylckama Vlieg JE. 2000. Characterization of the gene cluster involved in isoprene metabolism in *Rhodococcus* sp. strain AD45. J Bacteriol 182:1956–1963.
59. El Khawand M. 2014. Bacterial degradation of isoprene in the terrestrial environment. Dissertation. University of East Anglia, Norwich.
60. Smirnova GV, Oktyabrsky ON. 2005. Glutathione in bacteria. Biochem (Moscow) 70:1199–1211.
61. Zimmerling J, Tischler D, Grossmann C, Schlömann M, Oelschlägel M. 2017. Characterization of aldehyde dehydrogenases applying an enzyme assay with *in situ* formation of phenylacetaldehydes. Appl Biochem Biotechnol:1–13.
62. Fall R, Copley SD. 2000. Bacterial sources and sinks of isoprene, a reactive atmospheric hydrocarbon. Environ Microbiol 2:123–130.
63. Allocati N, Federici L, Masulli M, Di Ilio C. 2009. Glutathione transferases in bacteria. FEBS J 276:58–75.
64. Fahey RC, Brown WC, Adams WB, Worsham MB. 1978. Occurrence of glutathione in bacteria. J Bacteriol 133:1126–1129.
65. Johnson T, Newton GL, Fahey RC, Rawat M. 2009. Unusual production of glutathione in Actinobacteria. Arch Microbiol 191:89–93.
66. Allocati N, Federici L, Masulli M, Di Ilio C. 2012. Distribution of glutathione transferases in Gram-positive bacteria and Archaea. Biochimie 94:588–596.
67. Navarro-Llorens JM, Patrauchan MA, Stewart GR, Davies JE, Eltis LD, Mohn WW. 2005. Phenylacetate catabolism in *Rhodococcus* sp. strain RHA1: a central pathway for degradation of aromatic compounds. J Bacteriol 187:4497–4504.
68. Chen X, Kohl TA, Rückert C, Rodionov DA, Li L-H, Ding J-Y, Kalinowski J, Liu S-J. 2012. Phenylacetic acid catabolism and its transcriptional regulation in *Corynebacterium glutamicum*. Appl Environ Microbiol 78:5796–5804.
69. van Hylckama VJ, Janssen DB. 2001. Formation and detoxification of reactive intermediates in the metabolism of chlorinated ethenes. J Biotechnol 85:81–102.
70. Rui L, Kwon YM, Reardon KF, Wood TK. 2004. Metabolic pathway engineering to enhance aerobic degradation of chlorinated ethenes and to reduce their toxicity by cloning a novel glutathione *S*-transferase, an evolved toluene o-monooxygenase, and gamma-glutamylcysteine synthetase. Environ Microbiol 6:491–500.
71. Dorn E, Hellwig M, Reineke W, Knackmuss H-J. 1974. Isolation and characterization of a 3-chlorobenzoate degrading pseudomonad. Arch Microbiol 99:61–70.
72. Cooper DG, Goldenberg BG. 1987. Surface-active agents from two bacillus species. Appl Environ Microbiol 53:224–229.
73. Ames-Gottfred NP, Christie BR, Jordan DC. 1989. Use of the Chrome Azurol S agar plate technique to differentiate strains and field isolates of *Rhizobium leguminosarum* biovar *trifolii*. Appl Environ Microbiol 55:707–710.
74. Gordon D, Abajian C, Green P. 1998. Consed: a graphical tool for sequence finishing. Genome Res 8:195–202.
75. Gordon D, Green P. 2013. Consed. A graphical editor for next-generation sequencing. Bioinformatics 29:2936–2937.

76. Seemann T. 2014. Prokka: rapid prokaryotic genome annotation. Bioinformatics 30:2068–2069.
77. Krogh A, Larsson B, Heijne G von, Sonnhammer EL. 2001. Predicting transmembrane protein topology with a hidden Markov model: application to complete genomes. J Mol Biol 305:567–580.
78. Bertelli C, Laird MR, Williams KP, Lau BY, Hoad G, Winsor GL, Brinkman FS. 2017. IslandViewer 4. Expanded prediction of genomic islands for larger-scale datasets. Nucleic Acids Res. doi:10.1093/nar/gkx343.
79. Langmead B, Salzberg SL. 2012. Fast gapped-read alignment with Bowtie 2. Nat Methods 9:357–359.
80. Hilker R, Stadermann KB, Schwengers O, Anisiforov E, Jaenicke S, Weisshaar B, Zimmermann T, Goesmann A. 2016. ReadXplorer 2-detailed read mapping analysis and visualization from one single source. Bioinformatics 32:3702–3708.
81. Shevchenko A, Tomas H, Havlis J, Olsen JV, Mann M. 2006. In-gel digestion for mass spectrometric characterization of proteins and proteomes. Nat Protoc 1:2856–2860.
82. Al-Furoukh N, Ianni A, Nolte H, Hölper S, Krüger M, Wanrooij S, Braun T. 2015. ClpX stimulates the mitochondrial unfolded protein response (UPRmt) in mammalian cells. Biochim Biophys Acta 1853:2580–2591.
83. Rappsilber J, Mann M, Ishihama Y. 2007. Protocol for micro-purification, enrichment, pre-fractionation and storage of peptides for proteomics using StageTips. Nat Protoc 2:1896–1906.
84. Thakur SS, Geiger T, Chatterjee B, Bandilla P, Fröhlich F, Cox J, Mann M. 2011. Deep and highly sensitive proteome coverage by LC-MS/MS without prefractionation. Mol Cell Proteomics 10:M110.003699.
85. Cox J, Hein MY, Luber CA, Paron I, Nagaraj N, Mann M. 2014. Accurate proteome-wide label-free quantification by delayed normalization and maximal peptide ratio extraction, termed MaxLFQ. Mol Cell Proteomics 13:2513–2526.
86. Puigbo P, Guzman E, Romeu A, Garcia-Vallve S. 2007. OPTIMIZER: a web server for optimizing the codon usage of DNA sequences. Nucleic Acids Res 35:W126-W131.
87. Sambrook J, Russell DW (ed.). 2001. Molecular cloning. A laboratory manual, 3rd ed. Cold Spring Harbor Laboratory Press, Cold Spring Harbor, NY.
88. O'Connor KE, Dobson AD, Hartmans S. 1997. Indigo formation by microorganisms expressing styrene monooxygenase activity. Appl Environ Microbiol 63:4287–4291.
89. Warhurst AM, Clarke KF, Hill RA, Holt RA, Fewson CA. 1994. Metabolism of styrene by *Rhodococcus rhodochrous* NCIMB 13259. Appl Environ Microbiol 60:1137–1145.
90. Tischler D, Eulberg D, Lakner S, Kaschabek SR, van Berkel WJH, Schlömann M. 2009. Identification of a novel self-sufficient styrene monooxygenase from *Rhodococcus opacus* 1CP. J Bacteriol 191:4996–5009.
91. Dawson, R. M. C. 1986. Data for biochemical research, 3rd ed. Clarendon Press, Oxford.
92. Bradford MM. 1976. A rapid and sensitive method for the quantitation of microgram quantities of protein utilizing the principle of protein-dye binding. Anal Biochem 72:248–254.
93. Alonso S, Bartolomé-Martín D, del Álamo M, Díaz E, García JL, Perera J. 2003. Genetic characterization of the styrene lower catabolic pathway of *Pseudomonas* sp. strain Y2. Gene 319:71–83.

94. El-Said Mohamed M. 2000. Biochemical and molecular characterization of phenylacetate-coenzyme A ligase, an enzyme catalyzing the first step in aerobic metabolism of phenylacetic acid in *Azoarcus evansii*. J Bacteriol 182:286–294.
95. Kendall SL, Burgess P, Balhana R, Withers M, Bokum A ten, Lott JS, Gao C, Uhia-Castro I, Stoker NG. 2010. Cholesterol utilization in mycobacteria is controlled by two TetR-type transcriptional regulators: kstR and kstR2. Microbiology (Reading, Engl.) 156:1362–1371.
96. Nagy I, Schoofs G, Compernolle F, Proost P, Vanderleyden J, Mot R de. 1995. Degradation of the thiocarbamate herbicide EPTC (*S*-ethyl dipropylcarbamothioate) and biosafening by *Rhodococcus* sp. strain NI86/21 involve an inducible cytochrome P-450 system and aldehyde dehydrogenase. J Bacteriol 177:676–687.
97. Takeo M, Murakami M, Niihara S, Yamamoto K, Nishimura M, Kato D-i, Negoro S. 2008. Mechanism of 4-nitrophenol oxidation in *Rhodococcus* sp. strain PN1: characterization of the two-component 4-nitrophenol hydroxylase and regulation of its expression. J Bacteriol 190:7367–7374.
98. Beltrametti F, Marconi AM, Bestetti G, Colombo C, Galli E, Ruzzi M, Zennaro E. 1997. Sequencing and functional analysis of styrene catabolism genes from *Pseudomonas fluorescens* ST. Appl Environ Microbiol 63:2232–2239.
99. Wadington MC, Ladner JE, Stourman NV, Harp JM, Armstrong RN. 2009. Analysis of the structure and function of YfcG *from Escherichia coli* reveals an efficient and unique disulfide bond reductase. Biochem 48:6559–6561.
100. Mullins EA, Sullivan KL, Kappock TJ. 2013. Function and X-ray crystal structure of *Escherichia coli* YfdE. PLoS One 8:e67901.
101. Reverchon S, Nasser W, Robert-Baudouy J. 1994. pecS: a locus controlling pectinase, cellulase and blue pigment production in *Erwinia chrysanthemi*. Mol Microbiol 11:1127–1139.
102. Harris DR, Ward DE, Feasel JM, Lancaster KM, Murphy RD, Mallet TC, Crane EJ3. 2005. Discovery and characterization of a Coenzyme A disulfide reductase from *Pyrococcus horikoshii*. Implications for this disulfide metabolism of anaerobic hyperthermophiles. FEBS J 272:1189–1200.
103. Zhang CC, Huguenin S, Friry A. 1995. Analysis of genes encoding the cell division protein FtsZ and a glutathione synthetase homologue in the cyanobacterium Anabaena sp. PCC 7120. Res Microbiol 146:445–455.
104. Harth G, Maslesa-Galic S, Tullius MV, Horwitz MA. 2005. All four *Mycobacterium tuberculosis* glnA genes encode glutamine synthetase activities but only GlnA1 is abundantly expressed and essential for bacterial homeostasis. Mol Microbiol 58:1157–1172.
105. Gupta RS. 1994. Identification of a GroES (CPN10)-related sequence motif in the GroEL (CPN60) chaperonins. Biochem Mol Biol Int 33:591–595.
106. Hahn J-S, Oh S-Y, Roe J-H. 2002. Role of OxyR as a peroxide-sensing positive regulator in *Streptomyces coelicolor* A3(2). J Bacteriol 184:5214–5222.
107. Dhandayuthapani S, Zhang Y, Mudd MH, Deretic V. 1996. Oxidative stress response and its role in sensitivity to isoniazid in mycobacteria: characterization and inducibility of ahpC by peroxides in *Mycobacterium smegmatis* and lack of expression in *M. aurum* and *M. tuberculosis*. J Bacteriol 178:3641–3649.
108. Ramachandran S, Magnuson TS, Crawford DL. 2000. Isolation and analysis of three peroxide sensor regulatory gene homologs ahpC, ahpX and oxyR in *Streptomyces viridosporus* T7A--a lignocellulose degrading actinomycete. DNA Seq 11:51–60.

FIGURE LEGENDS

Fig. 1. Comparison of the styrene degradation cluster of *Gordonia rubripertincta* CWB2 with homologous clusters as found in the strains *Rhodococcus opacus* PD630 (Accession: NZ_CP003949) (22), *Rhodococcus* sp. AD45 (NZ_CM003191) (58), *Nocardioides* sp. Root240 (NZ_LMIT01000013), *Aeromicrobium* sp. Root495 (NZ_LMFJ01000002), *Rhodococcus* sp. ST-10 (AB594506) (13), *Rhodococcus opacus* 1CP (NZ_CP009112, NZ_CP009111) (48), *Pseudomonas* sp. Y2 (AJ000330) (38, 93) and *Sphingopyxis fribergensis* sp. Kp5.2 (CP009122) (17). Subclusters of strain CWB2 are indicated (S1-S4) and gene products are given in the legend coloured by their (predicted) function. Relevant homologous genes and clusters are emphasized by interspaced conjunctions. Clusteres of marked strains are reported to be involved in isoprene (●) or styrene (♯) degradation.

Fig. 2. Degradation of 4 mM *(S)*-styrene oxide with crude extract of styrene grown biomass of *Gordonia rubripertincta* CWB2 and 5 mM reduced glutathione (●). Only minor consumption was detected when excluding either reduced glutathione (○) or crude extract (X) from the reaction mix.

Fig. 3a. Proposed novel degradation pathway of styrene in *Gordonia rubripertincta* CWB2 (see text for details). **3b.** Proposed phenylacetic acid degradation pathway of *Gordonia rubripertincta* CWB2. The genes of the involved enzymes are present on the genome (cluster S4) and upregulated on transcriptome and the proteins on proteome level, respectively (see Table 2). Starting from the product of the upper degradation pathway, phenylacetic acid, strain CWB2 is able to metabolize styrene to acetyl-CoA or succinyl-CoA (adapted to 68).

TABLE LEGENDS

Table 1. Substrate spectra with focus on ones that might be related to styrene degradation in *G. rubripertincta* CWB2.

Table 2. Functional categorization of proteins from *G. rubripertincta* CWB2 that are supposed to be involved in styrene degradation and regulation on RNA and protein level. Enzymes and proteins with reported activity or function are underlined. For further details, see Dataset S1 in supporting material.

Table 3. Plasmids used in this study.

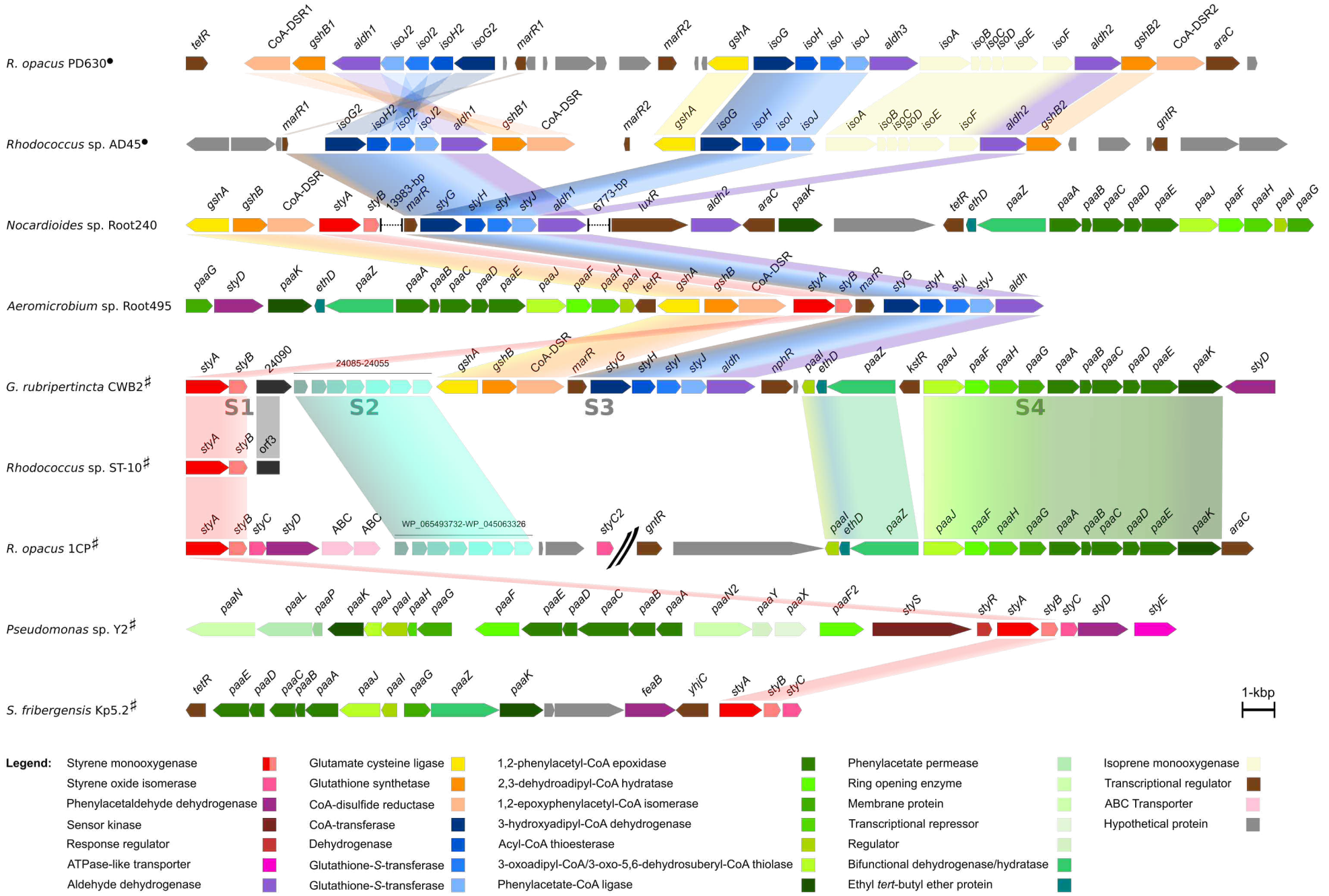
R. opacus PD630●
Rhodococcus sp. AD45●
Nocardioides sp. Root240
Aeromicrobium sp. Root495
G. rubripertincta CWB2#
Rhodococcus sp. ST-10#
R. opacus 1CP#
Pseudomonas sp. Y2#
S. fribergensis Kp5.2#
S1
S2
S3
S4
24085-24055
WP_065493732-WP_045063326
1-kbp
Legend:
Styrene monooxygenase
Styrene oxide isomerase
Phenylacetaldehyde dehydrogenase
Sensor kinase
Response regulator
ATPase-like transporter
Aldehyde dehydrogenase
Glutamate cysteine ligase
Glutathione synthetase
CoA-disulfide reductase
CoA-transferase
Dehydrogenase
Glutathione-S-transferase
Glutathione-S-transferase
1,2-phenylacetyl-CoA epoxidase
2,3-dehydroadipyl-CoA hydratase
1,2-epoxyphenylacetyl-CoA isomerase
3-hydroxyadipyl-CoA dehydrogenase
Acyl-CoA thioesterase
3-oxoadipyl-CoA/3-oxo-5,6-dehydrosuberyl-CoA thiolase
Phenylacetate-CoA ligase
Phenylacetate permease
Ring opening enzyme
Membrane protein
Transcriptional repressor
Regulator
Bifunctional dehydrogenase/hydratase
Ethyl tert-butyl ether protein
Isoprene monooxygenase
Transcriptional regulator
ABC Transporter
Hypothetical protein

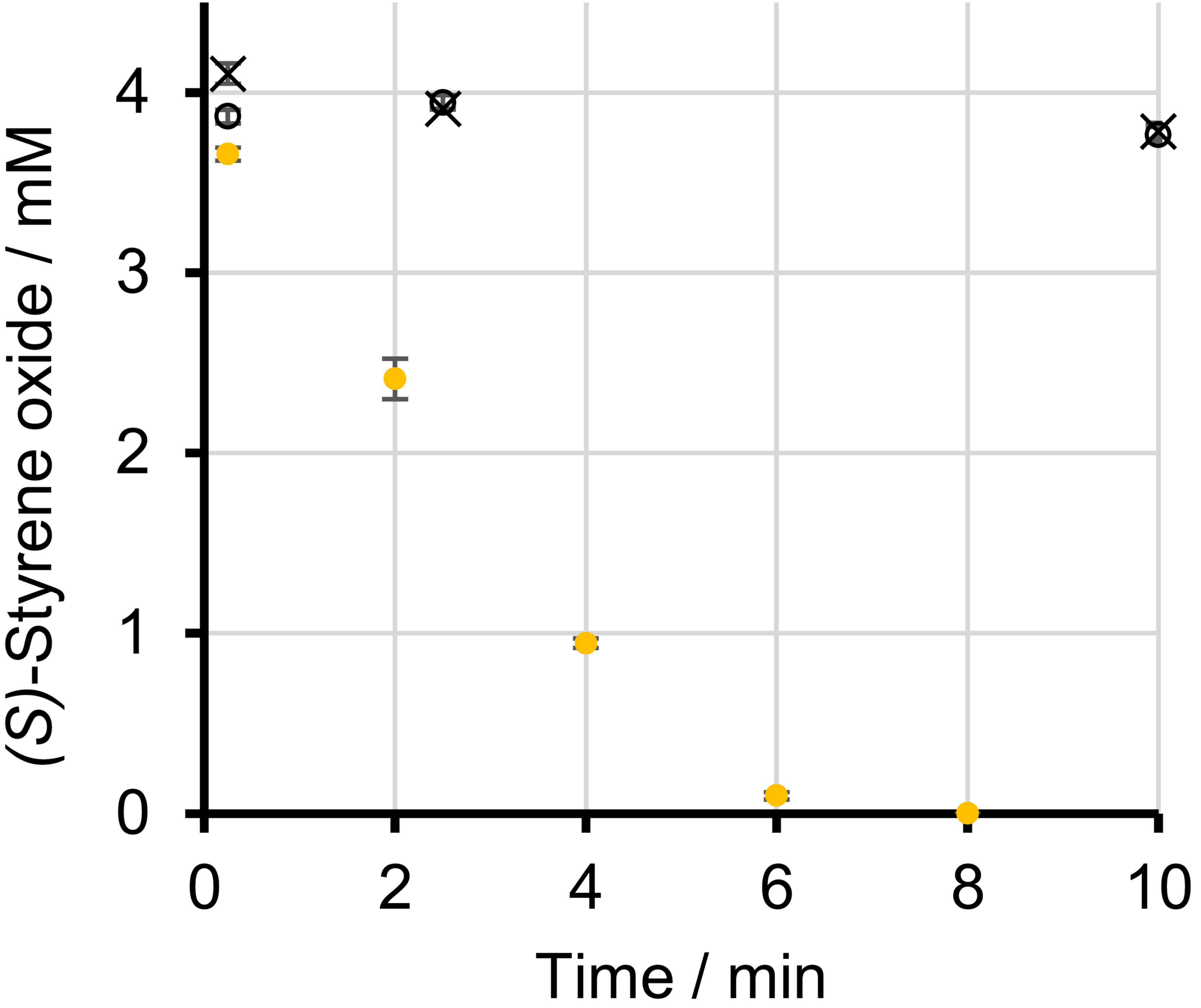
(S)-Styrene oxide / mM
0
1
2
3
4
0
2
4
6
8
10
Time / min

3a. Upper degradation pathway

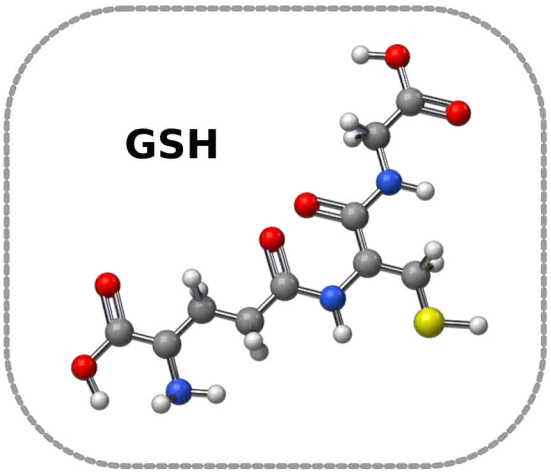

3b. Lower degradation pathway

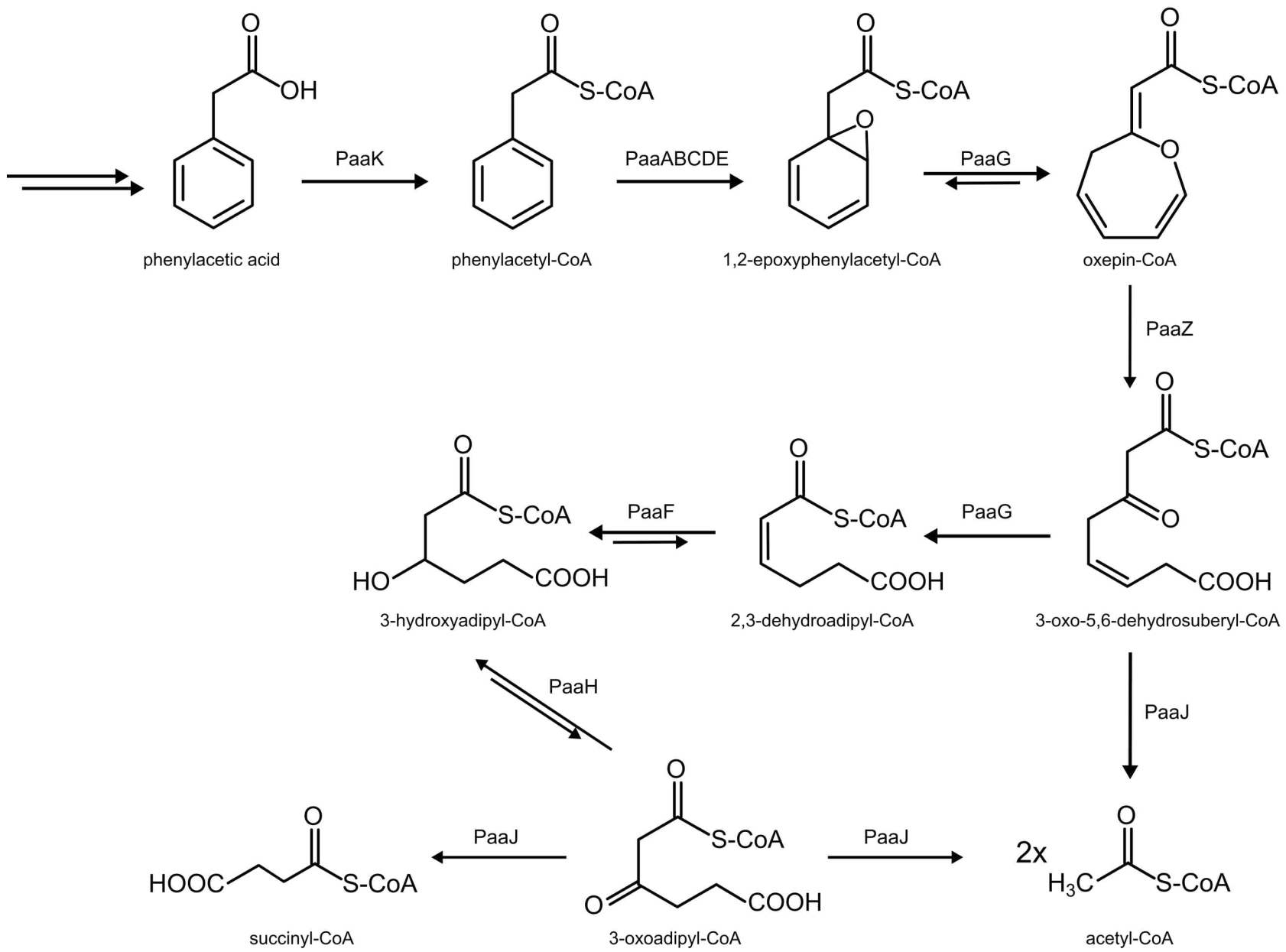

Table 1. Substrate spectra with focus on ones that might be related to styrene degradation in *G. rubripertincta* CWB2.

Substrate	Utilization
Styrene	++
Styrene oxide	++
2-Phenylethanol	++
Phenylacetaldehyde	++
Phenylacetic acid	+++
Succinate	++
Citrate	++
Isoprene	-
Mandelic acid	-
D-Fructose	+++

(+++) vigorous growth; (++) good growth; (+) growth; (-) no growth

726 **Table 2.** Functional categorization of proteins from *G. rubripertincta* CWB2 that are supposed to be involved in styrene degradation and regulation on RNA and protein
727 level. Enzymes and proteins with reported activity or function are underlined. For further details see supporting information.

Transcriptome				Proteome			Best hit on the Uniprot Database at amino acid level				
ORF	**Gene**	**A**	**M**	**Cyt**	**Mem**		**Name***	**Function**	**Accession**	**% Id**	**Reference**
23925	*styD*	7.7	8.6	7.1	5.7		*styD*	Phenylacetaldehyde dehydrogenase	BAL04135	76	(13, 50)
23930	*paaK*	8.1	6.0	8.1	5.9		*paaK*	Phenylacetate-coenzyme A ligase	Q9L9C1	68	(94)
23935	*paaE*	8.0	6.2	11.3	8.2		*paaE*	1,2-phenylacetyl-CoA epoxidase, subunit E	P76081	43	(8)
23940	*paaD*	8.1	6.7	NaNf	NaNf		*paaD*	1,2-phenylacetyl-CoA epoxidase, subunit D	P76080	42	(8)
23945	*paaC*	8.3	6.7	10.5	7.4		*paaC*	1,2-phenylacetyl-CoA epoxidase, subunit C	P76079	42	(8)
23950	*paaB*	8.0	6.8	8.8	9.1		*paaB*	1,2-phenylacetyl-CoA epoxidase, subunit B	P76078	67	(8)
23955	*paaA*	8.5	7.1	11.4	9.0		*paaA*	1,2-phenylacetyl-CoA epoxidase, subunit A	P76077	66	(8)
23960	*paaG*	7.7	7.4	6.9	6.8		*paaG*	1,2-epoxyphenylacetyl-CoA isomerase	P77467	37	(8)
23965	*paaH*	7.6	7.5	7.1	6.2	*S4*	*paaH*	3-hydroxyadipyl-CoA dehydrogenase	P76083	36	(8)
23970	*paaF*	7.1	7.4	7.1	5.8		*paaF*	2,3-dehydroadipyl-CoA hydratase	P76082	36	(8)
23975	*paaJ*	6.6	8.2	7.4	6.6		*paaJ*	3-oxoadipyl-CoA/3-oxo-5,6-dehydrosuberyl-CoA thiolase	P0C7L2	55	(8)
23980	*tetR*	7.3	1.8	2.7	1.8		*kstR2*	HTH-type transcriptional repressor KstR2	A0R4Z6	25	(95)
23985	*paaZ*	7.9	6.4	6.8	6.0		*paaZ*	bifunctional aldehyde dehydrogenase	P77455	51	(8)
23990	*ethD*	8.4	6.3	5.1	5.7		*ethD*	Uncharacterized 11.0 kDa protein	P43491	48	(96)
23995	*paaI*	7.3	5.2	NaNf	NaNf		*paaI*	Acyl-coenzyme A thioesterase PaaI	P76084	45	(8)
24000	partial	7.3	6.4	NaN	NaN			-	-	-	-
24005	*araC*	8.0	6.0	4.1	8.4		*nphR*	Transcriptional activator NphR	B1Q2A8	31	(97)
24010	*aldh1*	9.6	6.4	6.0	5.5		*styD*	Phenylacetaldehyde dehydrogenase	O06837	36	(98)
24015	*styJ*	10.1	6.1	7.7	5.9		*yfcG*	Disulfide-bond oxidoreductase YfcG	P77526	47	(99)
24020	*styI*	10.4	6.0	5.0	5.3		*isoI*	Glutathione-*S*-transferase	WP_045063292	49	(57)
24025	*styH*	9.5	6.3	5.0	4.8		*isoH*	1-hydroxy-2-glutathionyl-2-methyl-3-butene DH	WP_045063294	59	(57)
24030	*styG*	10.0	6.3	6.8	5.5	*S3*	*yfdE*	Acetyl-CoA:oxalate CoA-transferase	P76518	33	(100)
24035	*marR*	10.0	3.5	2.1	2.7		*marR*	regulatory protein	CAA52427	31	(101)
24040	*dsr*	9.1	4.7	8.5	4.8		*dsr*	Coenzyme A disulfide reductase	O58308	34	(102)
24045	*gshB*	8.9	4.9	5.7	3.8		*gshB*	Glutathione synthetase	P45480	50	(103)
24050	*gshA*	9.0	3.4	5.5	-2.2		*gshA*	Glutamate-cysteine ligase EgtA	P9WPK7	33	(104)

Table 2. (Continued)

24055	Hyp	7.8	8.5	NaNf	8.8	S2	-				
24060	Hyp	7.0	9.3	7.5	10.3		-				
24065	Hyp	6.6	9.3	8.8	10.3		-				
24070	Hyp	7.1	8.4	8.2	8.4		-				
24075	Hyp	6.8	9.5	7.9	8.2		-				
24080	Hyp	7.8	8.0	8.0	8.2		-				
24085	Hyp	9.2	10.7	5.8	6.2		-				
24090	Hyp	7.4	10.4	9.2	9.0		-	BAL04131	-	(13, 50)	
24095	*styB*	8.9	9.4	11.2	8.5	S1	*styB*	StyB-SMO flavin oxidoreductase	BAL04130	82	(13, 50)
24100	*styA*	9.0	9.1	8.1	6.0		*styA*	StyA-SMO styrene monooxygenase	BAL04129	86	(13, 50)
18380	*prmA*	5.3	3.5	3.4	3.2	Chromosome	*prmA*	propane monooxygenase hydroxylase large subunit	BAD03956	96	(25)
18385	*prmB*	3.1	4.8	4.9	2.0		*prmB*	propane monooxygenase reductase	BAD03957	80	(25)
18390	*prmC*	4.1	4.0	3.7	2.4		*prmC*	propane monooxygenase hydroxylase small subunit	BAD03958	85	(25)
18395	*prmD*	4.1	4.3	4.7	4.4		*prmD*	propane monooxygenase coupling protein	BAD03959	94	(25)
18400		3.7	3.7	4.9	2.3		-				
18405		3.3	3.8	NaNf	1.7		-				
18410	*adh*	3.5	3.8	3.4	1.5		*aldh1*	alcohol dehydrogenase	BAD03962	88	(25)
18415	*groL*	4.4	3.7	3.5	1.3		*groL*	60 kDa chaperonin	P28598	52	(105)
14195	*ahpD*	7.1	3.2	4.7	4.5		*ahpD*	Alkyl hydroperoxide reductase AhpD	Q50441	74	(106)
14190	*ahpC*	7.7	4.9	4.1	2.5		*ahpC*	Alkyl hydroperoxide reductase subunit C	A0R1V9	86	(107)
14185	*oxyR*	2.7	5.1	1.2	2.6		*oxyR*	Probable hydrogen peroxide-inducible genes activator	Q9X5P2	53	(108)

Transcript abundance (A) and fold-change (M) as well as protein fold-change in cytosol (Cyt) and membrane fraction (Mem) is given as log2 ratio. NaNf – not detected in the fructose proteome; NaN – not detected

731

Table 3. Plasmids used in this study

Plasmid	Relevant characteristic(s)	Source or reference
pET16bP	pET16b with additional multicloning site; allows synthesis of recombinant proteins with an N-terminal His_{10}-tag	U. Wehmeyer*
pEX-K2-pSGrA1	*GCWB2_24100* (1284-bp NdeI/NotI fragment) cloned into pEX-K2 vector	MWG Eurofins
pEX-K2-pSGrA2	*GCWB2_21620* (1359-bp NdeI/NotI fragment) cloned into pEX-K2 vector	MWG Eurofins
pEX-K2-pSGrD1	*GCWB2_23925* (1488-bp NdeI/NotI fragment) cloned into pEX-K2 vector	MWG Eurofins
pEX-K2-pSGrD2	*GCWB2_24010* (1437-bp NdeI/NotI fragment) cloned into pEX-K2 vector	MWG Eurofins
pSGrA1_P01	*GCWB2_24100* (1284-bp NdeI/NotI fragment) cloned into pET16bP	This study
pSGrA2_P01	*GCWB2_21620* (1359-bp NdeI/NotI fragment) cloned into pET16bP	This study
pSGrD1_P01	*GCWB2_23925* (1488-bp NdeI/NotI fragment) cloned into pET16bP	This study
pSGrD2_P01	*GCWB2_24010* (1437-bp NdeI/NotI fragment) cloned into pET16bP	This study

* personal communication